Int. J. Impact Engng Vol. 13, No. 1, pp. 1–20, 1993
Printed in Great Britain

0734–743X/93 $6.00 + 0.00

BALLISTIC IMPACT OF POLYCARBONATE—AN EXPERIMENTAL INVESTIGATION

S. C. WRIGHT, N. A. FLECK and W. J. STRONGE
Cambridge University Engineering Department, Trumpington St, Cambridge, CB2 1PZ, U.K.

(*Received* 10 *June* 1992; *and in revised form* 20 *August* 1992)

Summary—Polycarbonate is a polymer which is used for lightweight transparent armour in a wide range of applications. The material has an unusually high yield strain and ductility; this combined with a significant amount of strain hardening enables it to display impressive impact and perforation resistance. In this paper experimental observations are reported of penetration and perforation of polycarbonate plates by ballistic impact. Five mechanisms of deformation and subsequent fracture of the plate are identified. They are: elastic dishing, petalling, deep penetration, cone cracking and plugging. Thin plates impacted by spherical missiles exhibit elastic dishing, whereas thick plates suffer a deep penetration process. In both cases, final failure is by petalling. Cylindrical missiles impacting thick plates also cause deep penetration with final failure occurring by plugging. For thin plates impacted by cylindrical missiles, cone cracking develops from the leading edge of the missile. These process are described in detail, and the regime for each mechanism of failure is identified.

1. INTRODUCTION

Polycarbonate sheet or plate is used as a lightweight transparent armour for protection against missiles in the sub-ordnance velocity range in applications which range from safety goggles, industrial machine guards, aircraft windscreens and police riot shields. For higher speed missiles it is used in visors for bomb disposal personnel. Polycarbonate has superior impact and perforation resistance compared with other polymers, or indeed compared with some structural metals [1]. Despite the extensive use of polycarbonate in impact and safety applications, very little work has been conducted to investigate the penetration and perforation resistance of the material. Consequently there has been no real understanding of the material properties which give polycarbonate such good impact resistance. This paper reports experimental work undertaken to investigate and model the ballistic impact of polycarbonate.

The structure of the paper is as follows. First the ballistic rig and experimental techniques used are described briefly. The test programme is described in Section 3, and the experimental results are described at length in Section 4 for both missile types. Results of some simple quasi-static tests are also included. A comparison with the equivalent ballistic results for the impact of metals is made in Section 5. Theoretical analysis of the impact behaviour of polycarbonate is reported elsewhere [2], as is the characterization of the deformation and fracture behaviour of the material [3,4].

To avoid ambiguity, we define the following terms. The *distal face* of the plate is that parallel to, and farthest away from the impact face. *Dishing* is the flexural and stretching deformation of an annular region of the plate surrounding the missile impact point; in the dished region the middle surface is displaced normal to the surface of the plate. *Denting* is the localized indentation of the plate material under the common interface between the colliding missile and the plate; sometimes this is accompanied by *bulging* (also localized) on the distal face. *Penetration* is the embedding of the missile into the plate material, without a failure of the distal surface. It does not occur for thin plates, as failure of such plates occurs before the penetration process can become established. *Perforation* is the breaking through of the distal face of the plate by the missile. Perforation may follow

penetration. In all the tests in which perforation occurred, the whole missile passed through the plate.

2. EQUIPMENT AND TECHNIQUES

2.1. *Gas gun*

The purpose of the ballistic tests was to establish the modes of deformation and fracture of polycarbonate subjected to normal impact by either a spherical or flat nosed cylindrical missile over a wide range of impact velocities. The missile was propelled by a powerful single stage, high pressure nitrogen gas gun fired by the bursting of diaphragms; this triggering system gave a faster and more repeatable discharge than that obtained with electrically controlled valves. Missile velocities are measured before impact by the missile interrupting a light path. The gun was interfaced to a photographic system capable of producing high speed photographs of the impact event. The experimental apparatus also incorporated a high speed data logging facility.

Missile velocities before impact were measured using a purpose built timer connected to infra-red (IR) light beams passing through the gun barrel near the muzzle. There was some uncertainty ($\pm$ 5%) in the impact velocity resulting from a change in missile velocity during the sabot stripping process. However, this was offset by the requirement to limit the missile free flight distance between the muzzle and the target plate to a minimum, so reducing the problems of yaw and off-centre impact of cylindrical missiles. Missile exit velocities were estimated using a simple ballistic pendulum suspended immediately behind the plate. Thus, an approximate estimate was obtained for the energy absorbed during perforation.

2.2. *High speed photography*

An Imacon 790 high speed camera was used to photograph the impact event. The camera incorporates an electronic image intensifier which produced images on a phosphorescent screen. These images were then captured on Polaroid Type 42 film. Most of the impact work used framing speeds of 25,000 f.p.s. The camera produced up to eight full-frame images. In many of the tests the deformation was localized, so it was necessary to film close up details of the impact process (for example, field of view 30 $\times$ 20 mm). A simple adapter was made whereby any Pentax M42 screw fit lens could be fitted to the Imacon. A Tamron SP 60–300 zoom lens with a Pentax mount is now used and this, in conjunction with the bellows on the Imacon, allows a wide zooming ratio to be achieved.

Accurate triggering of the camera was crucial. A count-up count-down timer delay unit measured the speed of the missile and sabot together in the barrel near the muzzle, and then calculated the arrival time of the missile at the plate. This was done by charging a capacitor whilst the sabot travelled from the first IR beam to the second, at which instant, the capacitor was allowed to start discharging. The rates of charge and discharge were so arranged that their ratio was the same as the ratio of the distance between the two light beams, to the distance from the second beam to the plate. When the capacitor arrived at zero charge, a trigger pulse was sent to the camera.

Illumination for the camera was provided by a Metz Mecablitz 181 photographic flash unit, triggered by an earlier pulse from the timer delay unit, arranged such that the flash achieved its peak output when the camera was triggered.

Most of the dynamic photography was used to obtain images of the thinner plates viewed perpendicular to the line of motion of the missile, so that the profile of the plate at failure was obtained. Attempts were also made to film through the edge of the thick plates to see the development of damage inside the plate in the vicinity of the missile. Flats were milled in the edges of 12 mm thick plates to reduce optical distortion. The flats were polished using successively finer grades of carborundum paper (to 1200 grit), and then Hyprez diamond polishing compound. Flats were made on opposite sides so that the flash could be positioned on the far side of the plate, and facing the camera. This produced a white field in the photographs, with the missile and crack damage appearing in silhouette.

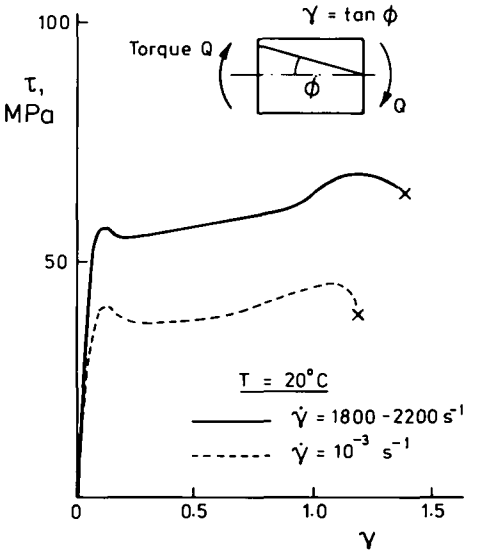

FIG. 1. Typical shear stress, shear strain responses of polycarbonate at low and high strain rate; tubular specimen loaded in torsion. Taken from Fleck *et al.* [3].

3. RESULTS

3.1. *Material properties*

The polycarbonate used in this study was Makrolon Type 281. The material is unusual in that it exhibits very large yield and fracture strains. Typical stress–strain responses in shear are shown in Fig. 1, for shear strain rates of $10^{-3}\,s^{-1}$ and $10^{3}\,s^{-1}$. These results were obtained with a thin-walled tubular specimen in a torsional Hopkinson bar experiment. The general form of the response is the same over a wide range of temperature and strain rate; indeed there is very little strain rate dependence. The yield and fracture strains are of the order of 0.1 and 1.5 respectively. The form of the curve is similar for tension, shear and compression, although it has been found experimentally that in general the yield stress in compression is typically 20% greater than that in tension. There is a more significant strain hardening characteristic in tension and compression compared with shear [4].

3.2. *Test programme*

The objective of the ballistic tests was to determine the mechanisms that were active in the failure of polycarbonate subjected to normal impact, and the regimes in which they occurred. Two types of missile were used. The flat ended cylinders were 7 mm in diameter and 9 mm long and made of silver steel. Cylindrical missiles suffer pronounced tumble in flight, leading to yawed impact. Efforts to eliminate this were not very successful. Consequently, most tests were conducted with missiles that consisted of 7 mm diameter steel ball bearings. The plates used were all of 2, 5 or 12 mm thickness. This allowed the effects of the ratio of missile diameter to plate thickness to be investigated. The plates were 104 mm in diameter and were simply supported. Impact velocities were varied from $160\,m\,s^{-1}$ at which a 7 mm diameter ball fails to perforate a 2 mm thick plate, to around $700\,m\,s^{-1}$ at which perforation of 12 mm thick plates can occur.

Quasi-static tests were conducted to investigate the dishing behaviour of thin plates. Circular plates of 2 mm thick polycarbonate of diameter D in the range $43\,mm < D < 132\,mm$ were loaded at their centre by either a flat or a hemispherical nosed punch; the punch diameter $2a$ was in the range $3.5\,mm < 2a < 14\,mm$. Force versus deflection plots and photographs of the deformed profile were obtained for punches pushed against freely supported plates.

4. BALLISTIC TEST RESULTS

The results of the ballistic tests are summarized in Fig. 2 for spherical missiles, and in Fig. 3 for cylindrical ones. The nominal missile velocity v is plotted against plate thickness h. The associated non-dimensional group $v(\rho/Y)^{1/2}$ and h/d are also given, where the density of polycarbonate is $\rho = 1200\,\mathrm{kg\,m^{-3}}$, the compressive uniaxial yield stress is $Y = 100\,\mathrm{MPa}$ (at a moderately high strain rate of $10^3\,\mathrm{s^{-1}}$), and d is the missile diameter. Inertia effects dominate the response when $v(\rho/Y)^{1/2} \gg 1$, while the response is quasi-static for $v(\rho/Y)^{1/2} \ll 1$. Here $v(\rho/Y)^{1/2}$ is of order unity, and inertia effects are considered in the indicated perforation processes. Each datum point in Figs 2 and 3 refers to a separate test. At any given thickness h, the missile is able to perforate the plate when its velocity exceeds the ballistic limit v_{50}. The ballistic limit is the mean minimum speed for perforation; this forms the boundaries illustrated in Figs 2 and 3.

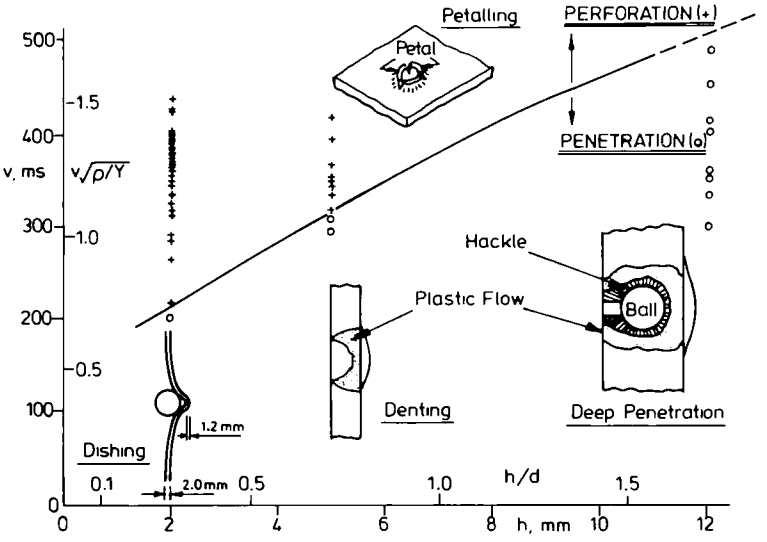

FIG. 2. Failure mechanisms for ballistic impact of polycarbonate by spherical missiles. (Hollow points indicate penetration, crosses indicate perforation.)

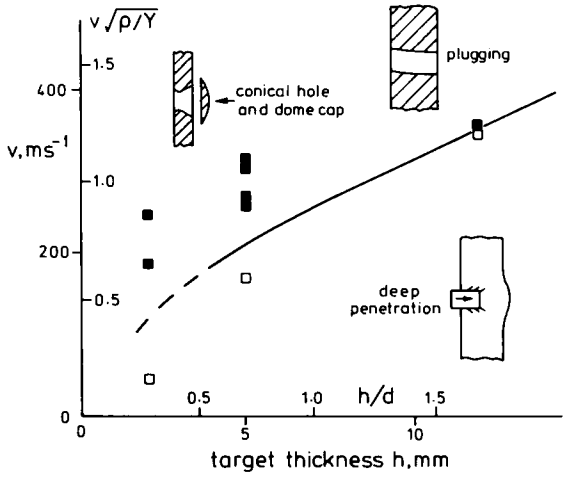

FIG. 3. Failure mechanisms for ballistic impact of polycarbonate by flat ended cylindrical missiles. (Hollow points indicate penetration, solid points indicate perforation.)

4.1. *Thickness* h = 2 *mm*

Quasi-static test. Consider first the quasi-static deformation of a 2 mm thick circular plate of polycarbonate loaded at its centre by a punch of hemispherical nose shape, Fig. 4(a). In the early stages of dishing, the specimen deforms principally by radial stretching into an almost straight sided cone. At larger punch displacements (u), localized yielding of the material in the contact region allows a more extreme deformation field and the specimen conforms to the punch nose shape. Outside this central region however, the specimen elastically deforms into a conical shape. At large deflections, there is a fairly marked transition between the central bulge and the conical portion of the specimen. This transition occurs away from the surface of the punch, at a radius of approximately $1.5a$–$2a$, giving rise to a curve in the deformed profile. The distribution of radial and hoop strain shortly before failure for the quasi-statically loaded specimen is shown in Fig. 4(b), as determined from measurements of a specimen marked with concentric circles.

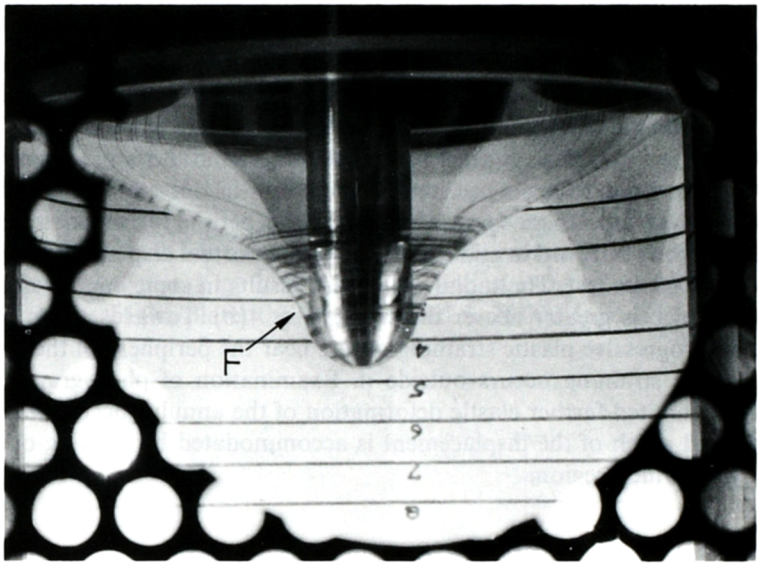

FIG. 4(a). Profile of quasi-statically deformed 2 mm thick plate near fracture for a round nosed indenter. $2a$ = 14 mm, d = 104 mm, displacement = 31 mm. "F" indicates the position of the fracture plane.

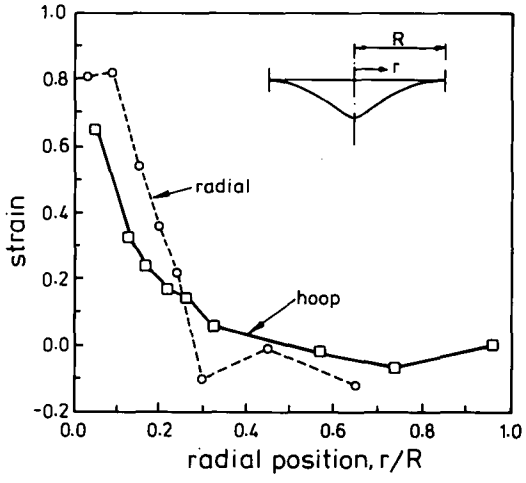

FIG. 4(b). Distribution of hoop and radial logarithmic strains in the plate [shown in Fig. 4(a)

As the displacement is increased, additional plastic deformation of the bulge in the contact area is accompanied by further elastic straining of the elastically deformed "cone". The plastic deformation involves the thinning of the material in this region. Eventually a point is reached where brittle fracture of the specimen occurs, generally along a circumferential section. The thickness of the material at the fracture surface has in most cases reduced to ~ 0.9 mm corresponding to a through thickness logarithmic strain of 0.8. The failure strain in the thickness direction does not vary appreciably with punch or specimen diameter. Examination of a specimen marked with concentric circles indicates that fracture occurs at or very near the point of inflexion of the deformed profile, that is just outside the contact zone [Fig. 4(a)]. A hemispherical cap is normally produced by the fracture. In a couple of cases, the failure was of a mixed mode type, being partly as just discussed and partly of a petalling nature (i.e. involving radial fracture).

A similar process occurs for *flat ended punches* with failure again occurring outside the contact region, although the "cap" produced is flat and has not permanently thinned in the contact region itself. In all cases the bulk of the specimen springs back to nearly a flat plate following fracture. A photograph of a specimen dished by a flat ended punch and near the point of failure is shown in Fig. 5.

The deformation response is generally one of elastic dishing of the bulk of the specimen together with localized plastic bulging for hemispherical nosed punches. The early response is predominantly elastic throughout the whole specimen. As the punch displacement is increased, yielding occurs in the contact zone. The material in the contact zone undergoes a small decrease in stress following yield, and the strain in this region rises sharply until strain hardening sets in. Except for material near the peripheral support ring, material elements move slightly outward in addition to the larger normal displacement which occurs during the course of the test. The radial movement results in some degree of hoop strain, the severity of which is greater nearer the centre, Fig. 4(b). Towards the latter stages of the dishing test progressive plastic straining occurs near the periphery of the contact zone, and further elastic straining occurs outside it. Examination of photographic sequences reveals that only limited further elastic deformation of the annulus occurs with increasing displacement, and much of the displacement is accommodated by necking or thinning of the plastically deformed region.

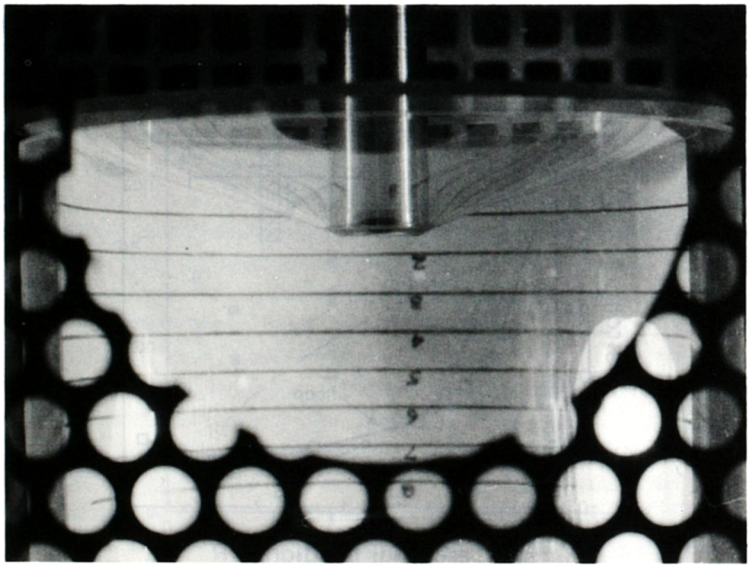

FIG. 5. Profile of quasi-statically deformed 2 mm thick plate near fracture for a flat nosed indenter. $2a = 14$ mm, $d = 104$ mm, displacement $= 13$ mm.

Consider the effect of nose shape. The stiffness of a specimen is greater for the flat ended indenter. The flat nose shape causes higher loads at a given displacement for all punch diameters, and fracture occurs at smaller displacements than for hemispherical nosed punches of the same diameter. The earlier fracture is readily explained by the stress concentration at the sharp corner of the flat ended punch.

In Fig. 6(a) we show the profiles at failure of 2 mm thick plates deflected by a round ended 7 mm diameter punch. The profile for the ballistic test is drawn from enlargements of high speed photographs. The plate deforms elastically into a straight sided cone with some plastic deformation concentrated in the centre. By contrast the profiles of plates hit ballistically are less straight sided and the dishing is more localized in the centre of the plate. This is caused by the inertia of the plate material.

Ballistic impact—spherical missiles. Now consider a spherical missile hitting the thinnest plate, $h = 2$ mm, by a ball of velocity $v < v_{50}$. The polycarbonate thins to as little as 0.8 mm where it is first impacted by the ball, and thereafter suffers dishing until the missile velocity is zero, whereupon some elastic recovery occurs. The plate retains some of its dished profile. Deformation is by a combination of bending and membrane stretching.

For velocities $v > v_{50}$ the polycarbonate dishes and then fails by petalling; that is, radial cracks propagate from the centre of the impact site. Scanning electron microscopy reveals that the cracks initiate at the centre of the impact site on the distal surface and then propagate through the thickness of the specimen and out in the radial direction. Triangular tongues or petals of polycarbonate are pushed in a radial direction by the missile until it can slip through the central hole. Similar behaviour also occurs in the impact of thin ductile metals such as mild steel [5,6]. Extensive elastic recovery of the plate starts to occur immediately after the ball has cleared the petals. A sequence of high speed photographs of these events is shown in Fig. 7(a), where the line of sight of the camera is obliquely across the rear face of the plate, the filming speed is 25,000 f.p.s., and missile motion is

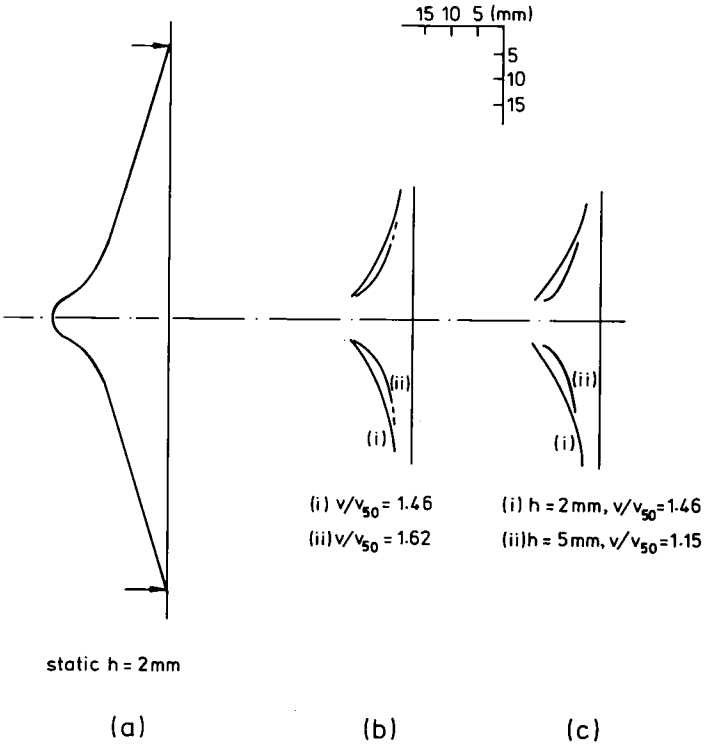

FIG. 6. Profiles of plates near fracture, (a) quasi-statically deformed, $h = 2$ mm, $2a = 7$ mm, (b) ballistic impact—effect of impact velocity, $h = 2$ mm, (c) ballistic impact—effect of plate thickness.

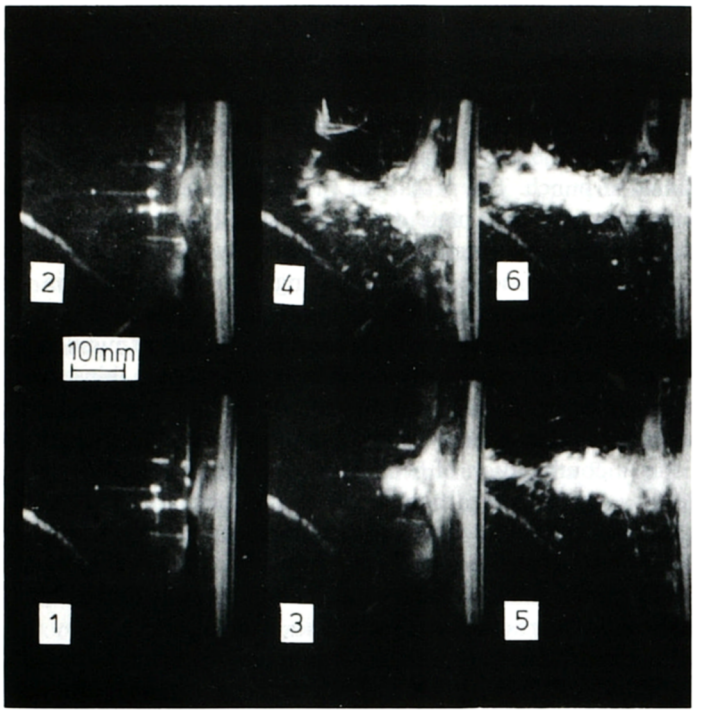

FIG. 7(a). Process of 7 mm diameter sphere perforating 2 mm thick polycarbonate plate. View across the distal face of the plate, missile motion from right to left, $v = 345\ \mathrm{m\ s^{-1}}$, $v/v_{50} = 1.62$, interframe period = 40 μs.

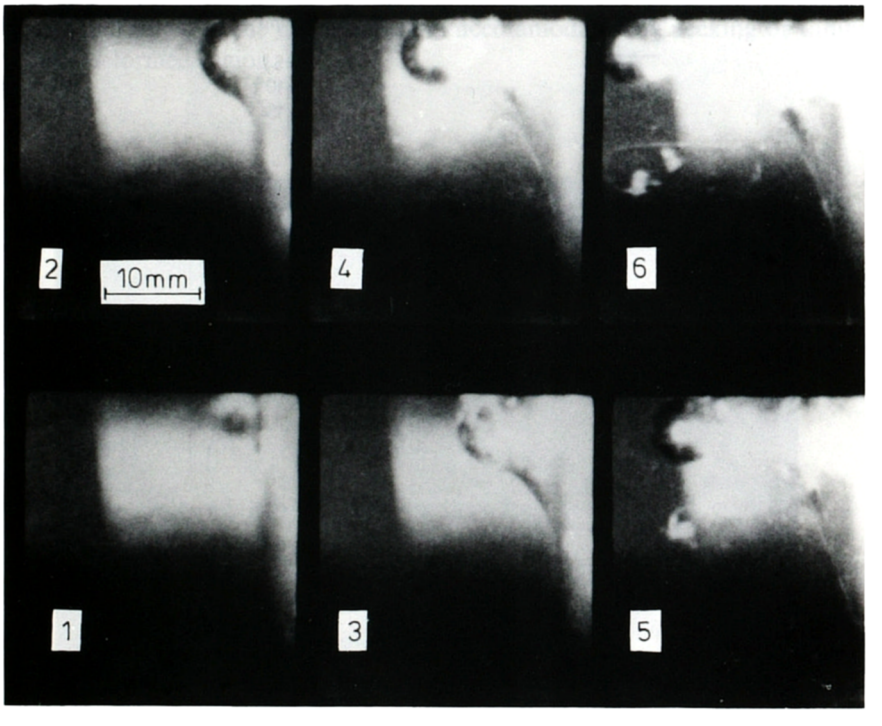

FIG. 7(b). Process of 7 mm diameter sphere perforating 2 mm thick polycarbonate plate. View across the distal face of the plate, missile motion from right to left, $v = 362\ \mathrm{m\ s^{-1}}$, $v/v_{50} = 1.70$, interframe period = 40 μs.

from right to left. A closer view of the impact event itself is seen in Fig. 7(b), where the line of sight is almost straight across the rear face of the plate. The perforated plates recover fully back to a flat plate except in the immediate vicinity of the impact site, where the petals become entangled and remain bent out of the plane of the plate (photograph in Fig. 8). Thus the petalling relieves the constraint in the central region of the plate, and allows greater elastic recovery back to a flat plate.

Scanning electron microscope (SEM) photographs of a petalled plate sectioned and polished after testing are shown in Fig. 9, which relates to a test where a 2 mm thick plate was hit at normal angle of obliquity by a ball at $v = 330\,\mathrm{ms}^{-1}$ (i.e. $v/v_{50} = 1.55$). In Fig. 9(a) a general oblique view of the sectioned surface is shown. The thinning of the material just off-centre is clearly visible. This thinning is also apparent from the high speed photograph in Fig. 7(b) frames 3 and 4, where the outer diameter of the polycarbonate surrounding the ball in frame 3 is only slightly larger than that of the ball itself (seen in

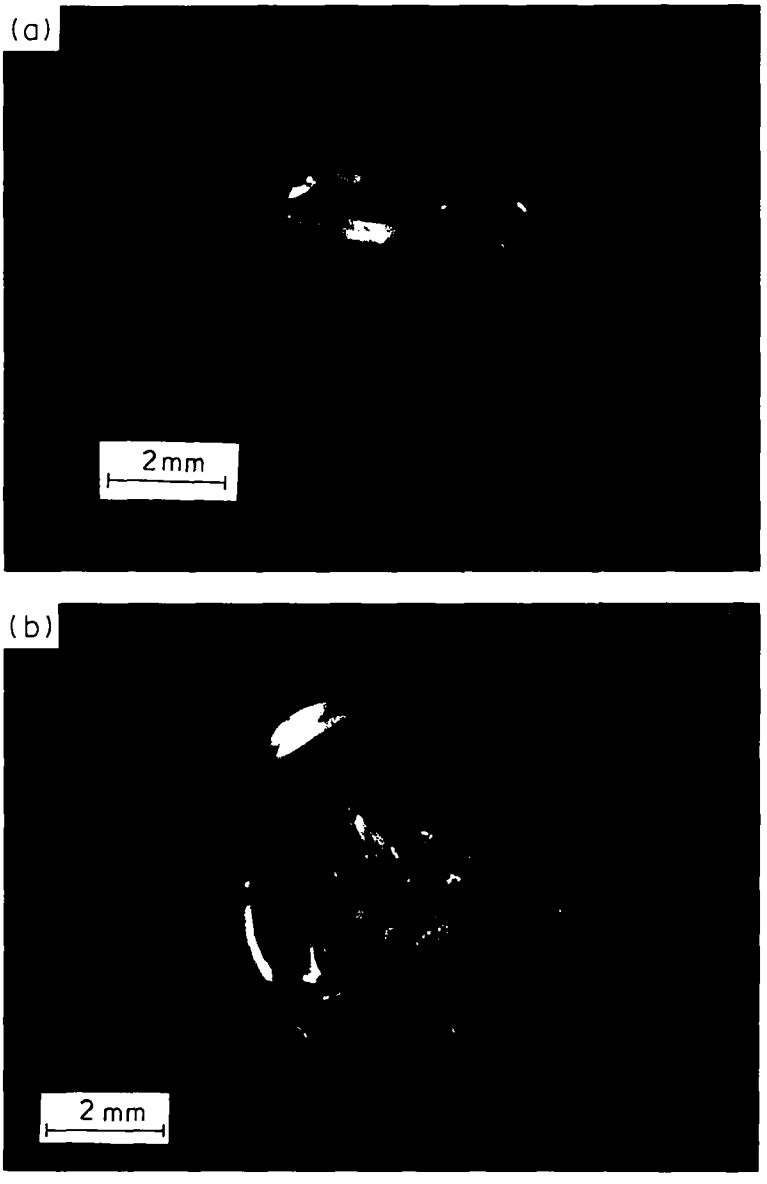

FIG. 8. Entangled petals in 2 mm thick plate after recovery, (a) side view and (b) plan view.

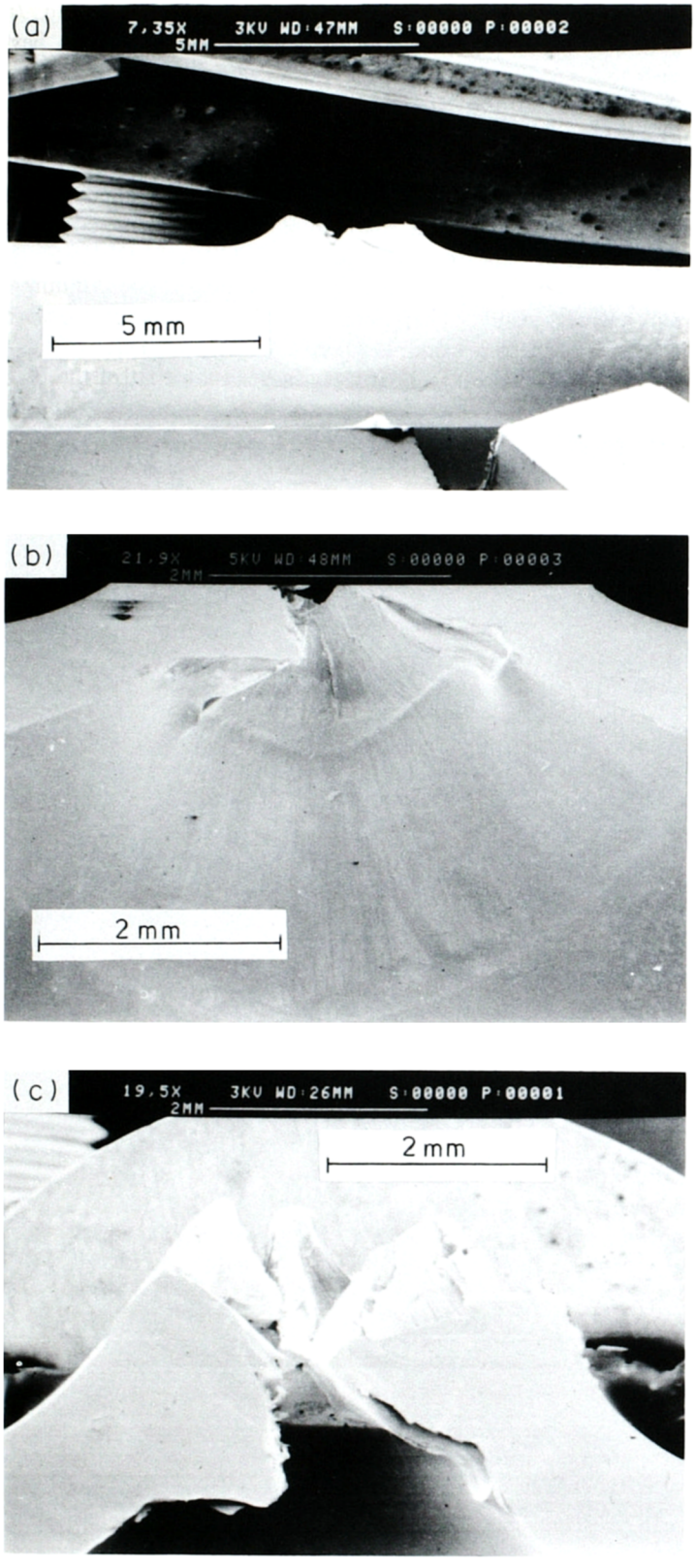

FIG. 9. Scanning electron micrographs of sectioned 2 mm thick plate showing petalled region after perforation by spherical missile, $v = 330\ \text{m s}^{-1}$, $v/v_{50} = 1.55$. (a) Oblique view of petalled region, (b) closer view of impact site, and (c) perpendicular view showing petal profiles.

frame 4). The resulting depression in the impact face is characterized by a series of fine striations, shown in greater detail in Fig. 9(b). The striations extend beyond the main depression past a vaguely defined lip onto the inner faces of the petals themselves. They are probably caused by sliding of the ball against the surface of the polycarbonate. A view perpendicular to the sectioned face, and showing the profile of the petals is shown in Fig. 9(c). Five petals are clearly identifiable in the half of the specimen displayed. The material at the centre (that is at the petal tips) has not thinned, and a ledge exists at the boundary between this central region, and the thinned area just outside it. Thus the sequence of events for $v > v_{50}$ is as follows. When the ball strikes the plate, there is a little plastic thinning due to indentation of the central region. Almost immediately this portion of the plate acquires the velocity of the missile and subsequently they move together. The material immediately surrounding the impact site connects the central portion with the bulk of the plate, and this annulus suffers bending and stretching as it wraps around the outer circumference of the ball. This is clearly visible in the high speed photographs in Fig. 7(b), where the "connecting" material lies almost parallel to the direction of missile motion. The thickness of the thinned section is 1.26 mm giving a through thickness logarithmic strain of 0.46.

The effect of impact velocity upon the deformation profile at fracture is shown in Fig. 6(b) for 2 mm thick plates impacted at $v/v_{50} = 1.62$. We observe that the higher impact velocity leads to perforation at smaller dishing displacements and to more localized deformation.

The petalling mechanism of final failure occurs for all sheet thicknesses investigated ($0.28 < h/d < 1.7$). The number n of petals produced is in the range 3–8, generally increasing with decreasing plate thickness. In none of the tests was the ball trapped by petals. Once the petalling process has initiated, it always continues until the missile has passed through the plate. Thus the petalling process itself appears to absorb only a small proportion of the total energy absorbed, with the major energy sink being the process which precedes petalling, either membrane dishing for thin plates, or deep penetration of thick ones.

Ballistic impact—cylindrical missiles. For $h = 2$ mm perforation occurs by the propagation of a conical crack through the thickness of the plate. Examination of fracture surfaces by scanning electron microscopy reveals that the crack initiates at the leading edge of the missile and propagates through the thickness of the plate to the distal face. For $v < v_{50}$ elastic dishing occurs.

4.2. *Thickness* h = 5 *mm*

Ballistic impact—spherical missiles. Now consider the ballistic impact of plates of intermediate thickness, $h = 5$ mm by spherical missiles. The response is intermediate between those of the thick and thin plates. For $v < v_{50}$, little dishing occurs, leaving the plate with a generally flat profile except at the impact site. The thickness is inadequate to allow a deep penetration process to become established and denting results, producing a depression which is of slightly smaller diameter than the ball. This depression has a pointed shape caused by radial elastic recovery. A zone of yielded material appears around and ahead of the missile. Bulging again occurs on the distal face of the plate, and some very small scale cracking or hackle is visible at the tip of the indentation (see Fig. 2). For velocities $v > v_{50}$, some dishing occurs prior to failure, which is again by petalling. High speed photographs of the event are shown in Fig. 10, for which the filming speed is 25,000 f.p.s. Here the impact has occurred between frames 1 and 2, and the ball is breaking clear of the plate in frame 5. In this test a trail of debris resulting from disintegration of the sabot can be seen passing through the plate in the wake of the ball. The lack of extensive dishing, and the local nature of the bulge on the rear face of the plate are evident, compared with the more extensive dishing of the thinner plates (Fig. 7). This is also illustrated in Fig. 6(c) where profiles at failure are shown for $h = 2$ mm $v/v_{50} = 1.46$ and $h = 5$ mm $v/v_{50} = 1.15$. The bulge is caused more by denting of the plate as noted above, rather than dishing. Elastic recovery of the limited dishing takes place after perforation. The number of petals n produced tends to be fewer than for $h = 2$ mm, typically $n = 4$.

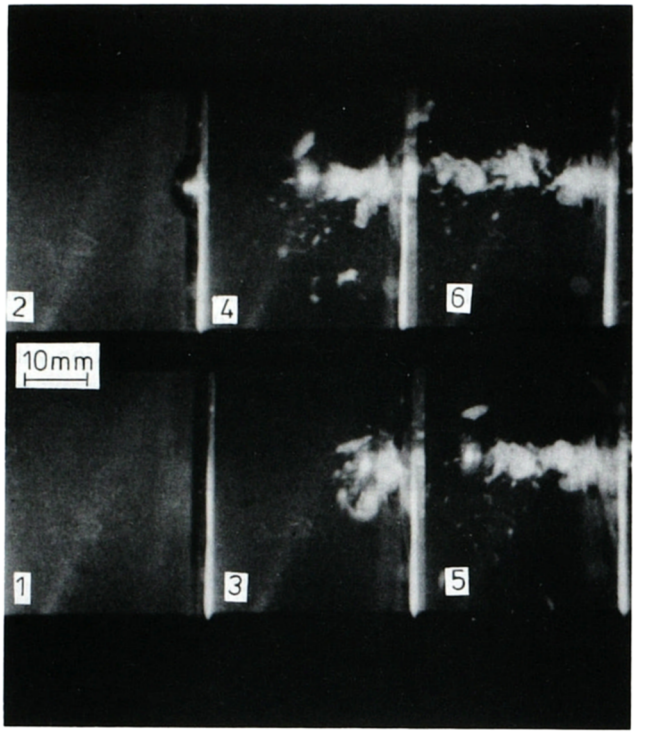

FIG. 10. Process of 7 mm diameter sphere perforating 5 mm thick polycarbonate plate. View across the distal face of the plate, missile motion from right to left, $v = 333\ \text{ms}^{-1}$, $v/v_{50} = 1.05$, interframe period = 40 μs.

The denting of the plate is clearly visible after the test. We show in Fig. 11(a) an SEM photograph of a polished section of the specimen relating to Fig. 10. The angle of view is obliquely across the section, viewing from the impact side. The thickness of the material in the dented region is approximately 4 mm. The degree of thinning is considerably less than for $h = 2$ mm because the very marked stretching of the material wrapped around the missile as shown in Fig. 7(b) does not occur for $h = 5$ mm. However, flexure around the missile nose is more important for the thicker plate, leading to substantial bending strains at the distal surface. This enables fracture to again be initiated at the distal surface, and to propagate through the thickness of the specimen, whilst at the same time propagating out in the radial direction to produce triangular petals. Thus, the mechanism of failure is similar for both the thin and intermediate thickness plates, although the deformation mechanism which precedes it is slightly different. The interpretation that the fracture is controlled by a critical failure strain in the distal surface of the plate is supported by the fact that the central plate displacement at failure is similar for both static and dynamic cases [Fig. 6(a)]. Closer views of the fracture surface for $h = 5$ mm are shown in Figs 11(b), (c) and (d). There is some evidence of material melting in Fig. 11(d).

Ballistic impact—cylindrical missiles. Now consider the impact of 5 mm thick polycarbonate plates by circular cylinders, as shown in Fig. 3. For $v < v_{50}$, denting occurs on the impact face accompanied by bulging on the distal face. The missile bounces off the plate leaving a depression approximately 10% smaller in diameter than the missile.

Now consider $v > v_{50}$. A finite time after impact (say 4 μs), the specimen will have deformed locally (an elastic shock wave moving out in a radial direction will have travelled approximately 8 mm in this time) as in Fig. 12(a). The central part of the specimen is now dished, and a brittle fracture may occur across a flat plane as shown. This results in the conical hole and dome shaped cap observed following elastic recovery [Figs 12(b) and (c)].

Consider the cone shaped hole [Fig. 12(c)]. The proportions of the damage vary with

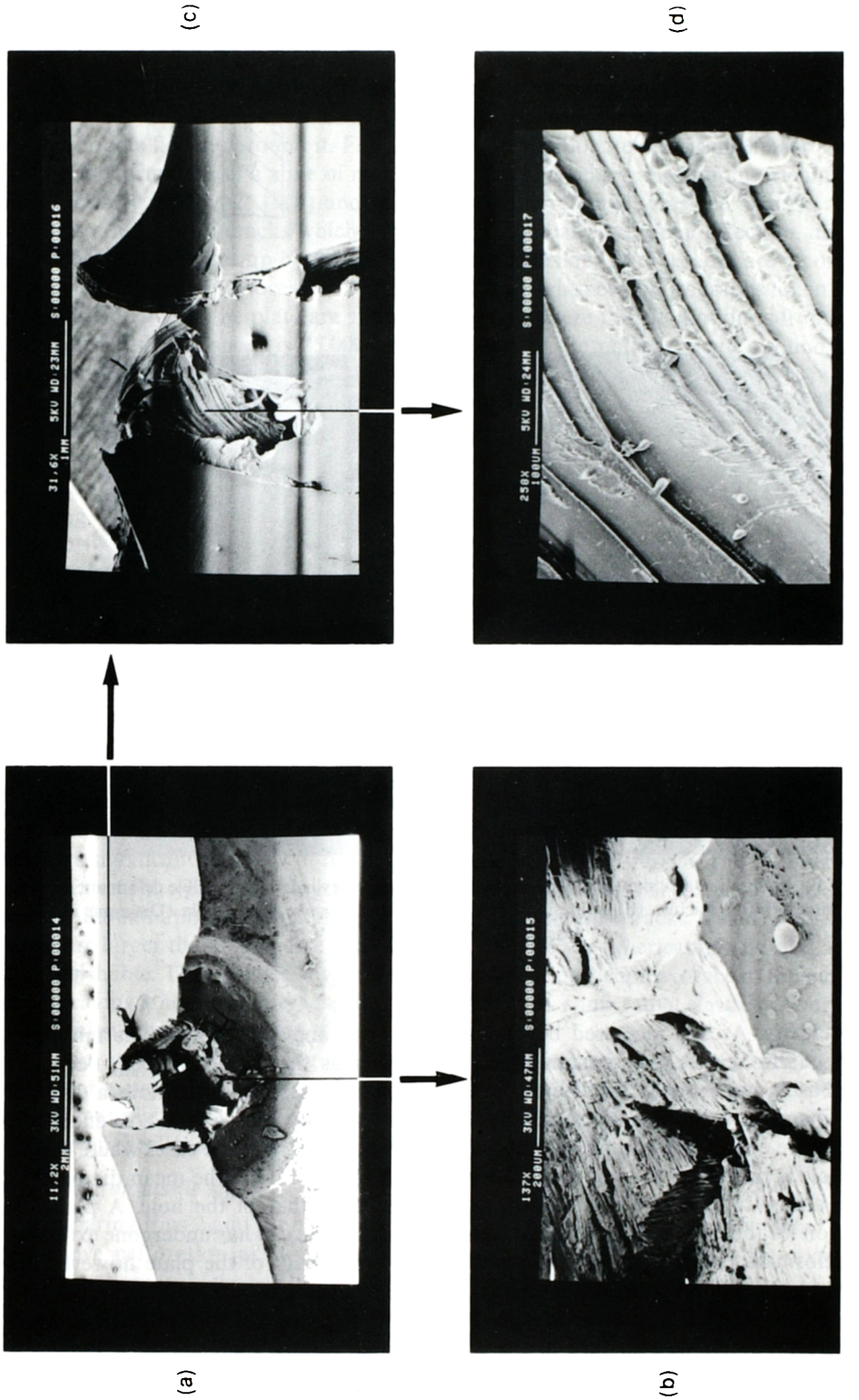

FIG. 11. Scanning electron micrographs of sectioned petalled plate, $h = 5$ mm, $v/v_{50} = 1.05$. (a) Oblique view of impact face showing residual dent, (b), (c) closer views of petal fracture surfaces, and (d) close-up of fracture surface.

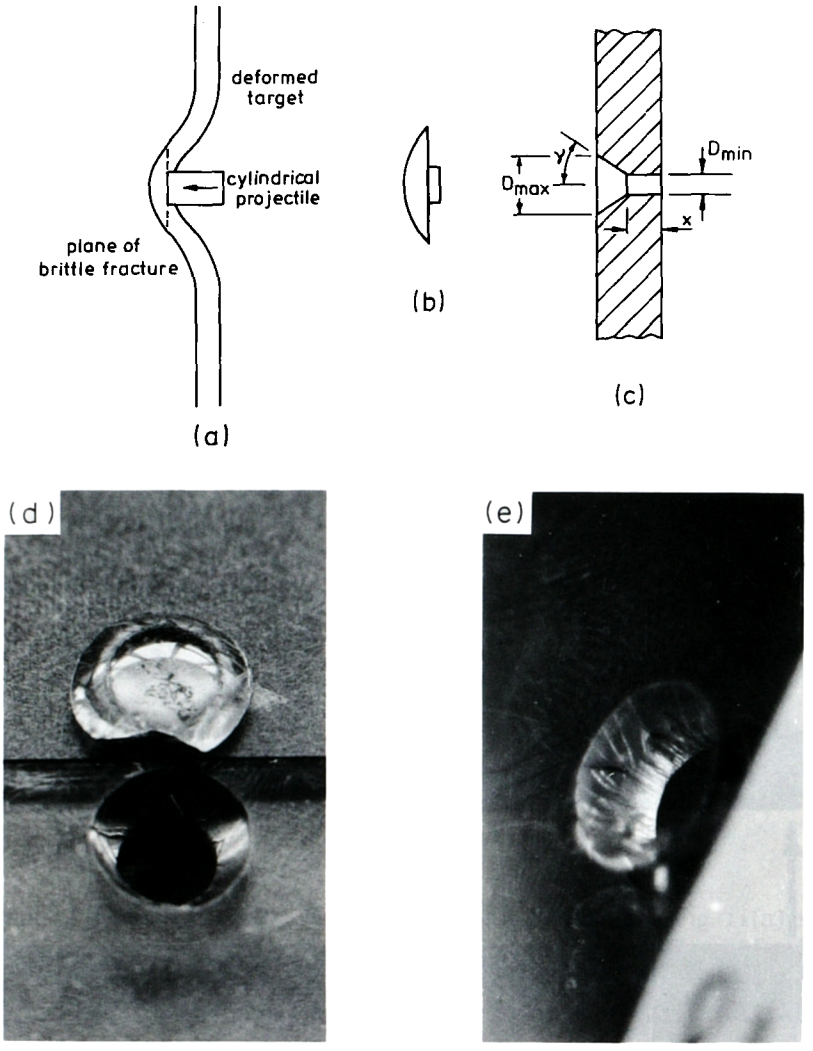

FIG. 12. Perforation of 5 mm thick plate impacted by flat ended cylinder. (a) Possible deformation at onset of brittle fracture, (b)–(d) residual hole and cap, and (e) cone shaped hole. (Diagrams in this figure are not to scale).

impact velocity. As v is increased beyond v_{50}, the cone angle γ reduces. The minimum diameter of the hole D_{min} is reasonably constant whereas the maximum D_{max} decreases with increasing impact velocity. There is a short cylindrical section to the hole, a distance x, which increases with impact velocity. As the impact velocity rises, so the hole effectively becomes more cylindrical as a plugging type failure dominates. For the cases where a cone shaped hole is produced, a dome shaped cap is ejected [Fig. 12(b)] the mean diameter of which is about 15 mm, which is considerably larger than that of the hole. A plausible justification for the nature of the damage is that material in the cap has undergone extensive plastic deformation, so it retains its deformed shape. The bulk of the plate however has deformed elastically, and the strain energy so stored is sufficient to enable the plate to recover back to its flate state even though the material near the hole has undergone some plastic deformation. The rear face of the hole recovers from a diameter of 15 mm to a diameter of 11 mm. Photographs of a hole and cap are shown in Figs 12(d) and (e). At substantially higher impact velocities plugging becomes established before the plate can dish sufficiently for the cone shaped hole to be produced, resulting in rough sided cylindrical holes.

4.3. *Thickness* h = 12 *mm*

Ballistic impact—spherical missiles. Consider next the thickest plate, $h = 12$ mm, hit at normal obliquity by a ball at $v < v_{50}$. The ball penetrates the plate, but does not perforate it. Bulging occurs at the rear surface. Examination of the plate through its polished side wall reveals that a region around the penetrating missile undergoes shear yielding as plate material flows around the periphery of the missile [see Figs 13(a) and (c)]. This region is sharply defined as the polycarbonate undergoes a change in refractive index when it yields. Thus the ball penetrates the plate by a deep penetration process, with the polycarbonate flowing around it. Failure of the polycarbonate occurs at the surface of the ball by the formation of a zone of many small tensile cracks with random orientations, as shown clearly in Figs 2, 13(b) and (c). This zone is referred to as the "hackle zone". It contains a number of cracks which run out from the ball in a radial direction, due to the tensile hoop stresses set up by the axisymmetric expansion. These cracks are incorporated in the modelling of this process by Wright *et al.* [2]. High speed photographs taken through the polished edge of the plate are shown in Fig. 14, where missile motion is from right to left, and the filming speed is 25,000 f.p.s. The flow of the polycarbonate around the ball combined with elastic recovery results in the hole behind the missile being of only 2 mm diameter, that is 70% less than that of the ball. The surface of the hole is rough due to the hackle. The photographs in Figs 13(c) and (d) show the damage for a case where the impact velocity is just less than v_{50}. A spiral crack can be seen emanating from the missile towards the distal surface of the plate. For $v > v_{50}$, final failure of the plate is again by petalling.

In early tests with no high speed photographs, it was not clear if the cracking ahead of the missile occurs during penetration, or due to an unloading effect as the missile comes to rest. The high speed photographs taken through the edge of the plate and discussed above suggest that the cracking may occur during penetration. The overall process of penetration of thick plates appears to be one of deep penetration, preceded and succeeded by transients associated with the missile being near to a free surface. Observation of this behaviour is novel. In particular, for the impact of thick metal plates there is much less elastic recovery of the material behind the missile, and the final hole size is larger than that of the ball.

Ballistic impact—cylindrical missiles. Now consider impact of the thick plates, $h = 12$ mm by cylindrical missiles. For $v < v_{50}$, axisymmetric expansion and deep penetration occur similar to that for a ball, although the greater length of the cylinder prevents significant recovery of the polycarbonate behind the missile. The cylinder indents the surface of the plate, causing bulging on the distal face, and shear yielding around the missile. Examination through the edge of the plate reveals cracks ahead of the missile. These are larger than the hackle cracks associated with the spherical missile, and are more distinguishable. The cylinder always bounces back out of the impact face of the penetrated plates leaving a hole of about 5.5 mm in diameter. Thus, some radial elastic recovery occurs as the missile leaves the plate.

For $v > v_{50}$ a shear plugging type failure takes place, similar to that experienced in the impact of metal plates. Shear yielding is still apparent around the missile and a distorted plug of material is expelled from the plate. The fracture surface of the hole features a large number of parallel striations running along the hole (see Fig. 15).

4.4. *Effect of missile shape*

Comparing Figs 2 and 3 we observe that the ball requires a significantly higher velocity to achieve perforation of any given thickness for the range of thicknesses investigated. However, the mass of the ball (1.4 g) is considerably less than that of the cylinder (2.8 g).

For small h/d and for both missile types, the principle energy dissipating mechanism is elastic dishing. The dishing is brought to an end by a fracture event at the contact site, either petalling initiated at the distal surface for spherical missiles or cone cracking which initiates from the leading edge of cylindrical missiles. In both cases the final fracture absorbs little energy and appears to occur at a degree of dishing which does not depend upon missile type. For large h/d penetration occurs by a deep penetration mechanism which is

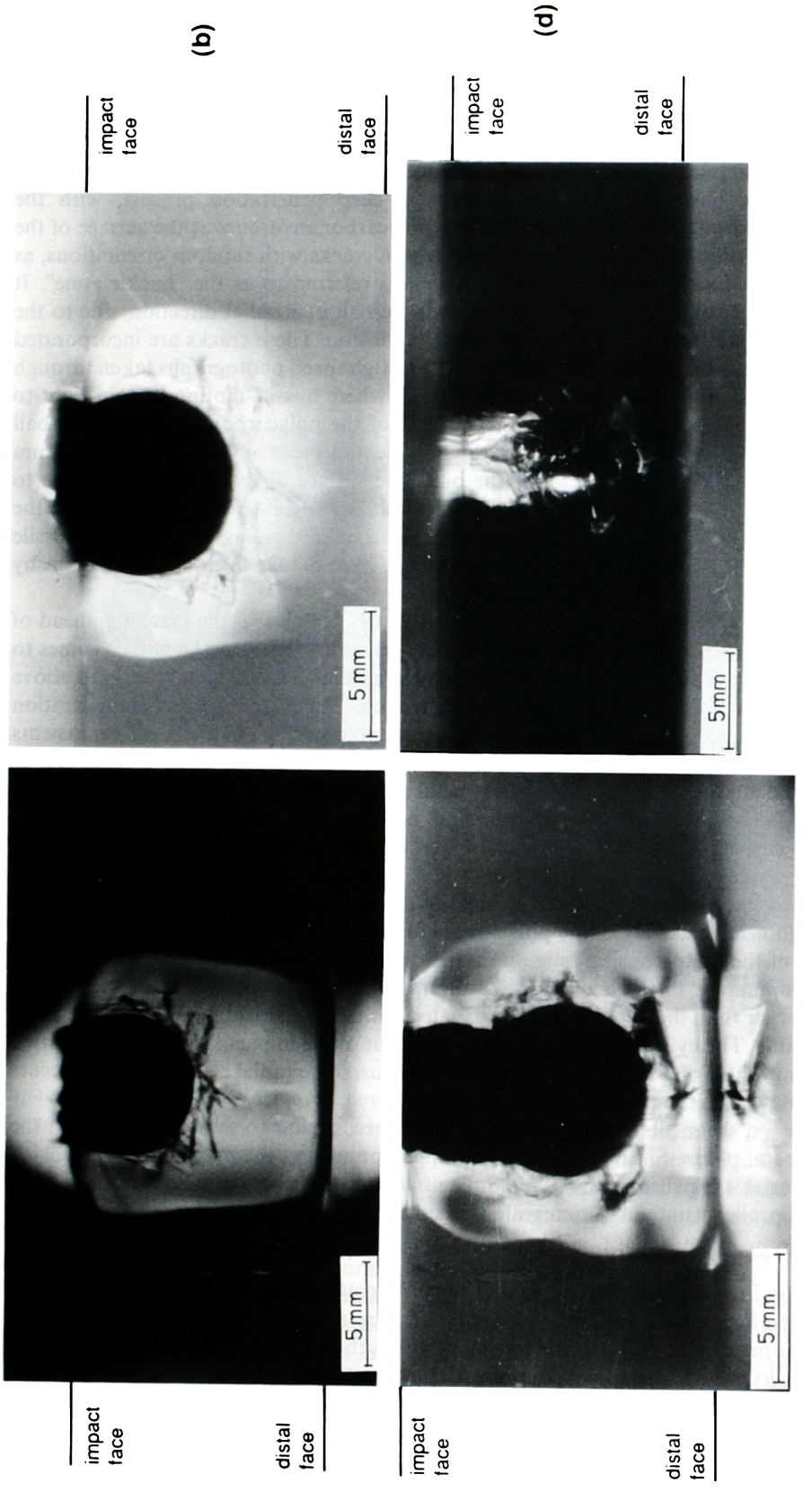

FIG. 13. Spherical missile embedded in thick plate after test, ball motion from top to bottom. (a) Failure of PC at missile surface to generate hackle, $v/v_{50} = 0.8$, (b) zone of plastic deformation around missile, $v/v_{50} = 0.8$, (c) zone of plastic deformation around missile, hackle also visible, $v/v_{50} = 0.82$, and (d) spiral crack running from missile towards distal face of plate. Hackle compressed into wake of missile also visible, $v/v_{50} = 0.82$.

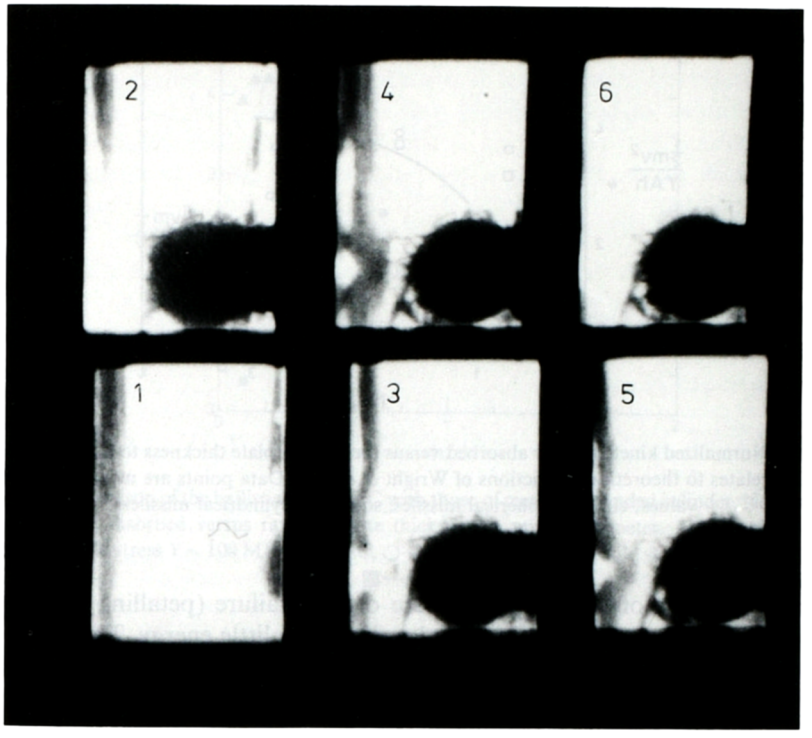

FIG. 14. Process of 7 mm diameter sphere perforating 12 mm thick PC plate. View through the polished edge of the plate, missile motion from right to left, $v = 298$ m s^{-1}, $v/v_{50} = 0.60$, interframe period = 40 μs.

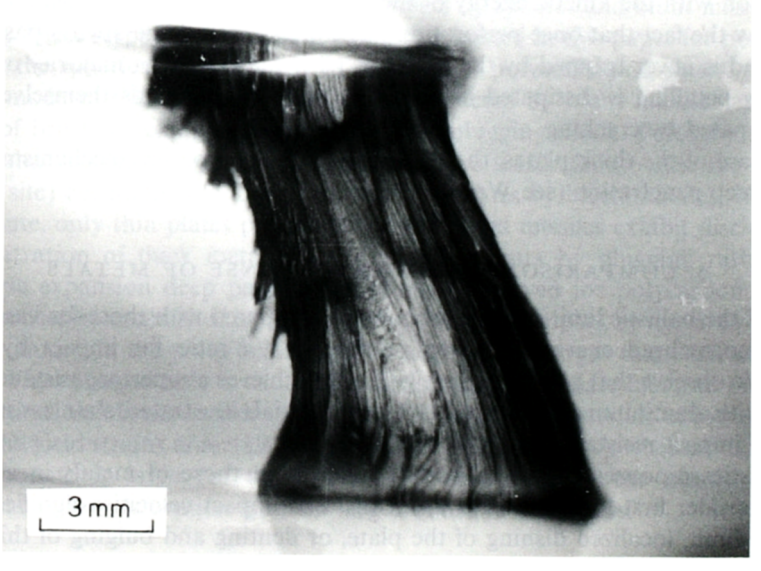

FIG. 15. A 12 mm thick PC plate perforated by flat nosed cylindrical missile. View through the polished edge after test showing corrugations in fracture surface, $v > v_{50}$, missile motion from top to bottom.

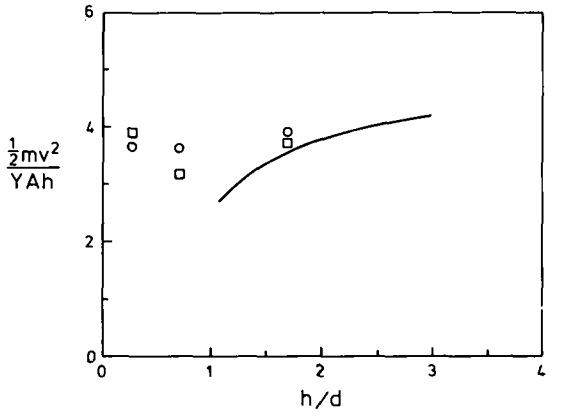

FIG. 16. Normalized kinetic energy absorbed versus the ratio of plate thickness to missile diameter. The line relates to theoretical predictions of Wright *et al.* [2]. Data points are mean experimental values; circles—spherical missiles, squares—cylindrical missiles.

similar for both types of missile. The nature of final failure (petalling versus plugging) again depends on the type of missile, but also dissipates little energy. Thus, for missiles of similar mass, the nose shape does not affect the ballistic limit (Fig. 16).

Wright *et al.* [2] have modelled the process of deep penetration of polycarbonate as occurs when a thick plate is penetrated by either missile shape. The predictions of the model are superimposed upon experimental data for both missile shapes in Fig. 16. This model only applies to thick plates where $h/d > 1$.

4.5. *Comment on energy dissipation*

Of the five failure mechanisms observed in the penetration and perforation of polycarbonate, only two appear to be significant as energy processes. For the case of thin plates the majority (typically 80–90%) of the energy dissipated is absorbed by elastic dishing. The final failure processes are petalling for spherical missiles or cone cracking from the leading edge for flat ended cylinders; in both cases the fracture energy is small in comparison with the kinetic energy of the colliding missile at the ballistic limit. This is supported by the fact that once perforation has started, the missile always passes through the plate, and is never trapped by the petals or plate material. The majority of the energy absorbed by petalling is dissipated in plastic bending of the petals themselves, and very little is dissipated by cracking.

For the case of the thick plates, the principal energy dissipation mechanism appears to be that of deep penetration (see Wright *et al.* [2]).

5. COMPARISON WITH THE RESPONSE OF METALS

In Fig. 17 the ballistic limit of polycarbonate is compared with those for various metals, plotted as normalized energy absorbed versus the h/d ratio for impact by flat ended cylinders. We observe that polycarbonate generally achieves a superior resistance to impact compared with aluminium and mild steel. Of the materials illustrated, stainless steel displays the greatest impact resistance.

The ballistic responses of polycarbonate differ from those of metals in a number of respects. Consider first the behaviour of metals. For impact velocities significantly below the ballistic limit, localized dishing of the plate, or denting and bulging of thicker plates, generally occurs. As the impact velocity is increased, the degree of dishing increases with impact velocity for impact velocities below that for perforation. Further increases in impact velocity above the ballistic limit result in perforation at a smaller degree of dishing. At very high velocities, the damage is very localized around the impact site. These observations

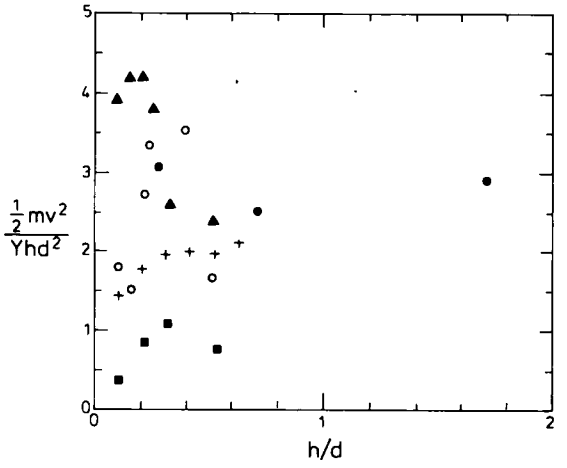

FIG. 17. Comparison of the ballistic limit of PC with those of metals, flat ended cylinder. Normalized kinetic energy absorbed versus ratio of plate thickness to missile diameter. At a strain rate of $10^3\,s^{-1}$ the yield stress $Y \sim 100$ MPa; ●—PC, ○—mild steel [7], +—mild steel [8], ▲—stainless steel [7], ■—aluminium (7].

are general [9] and are described in detail by Lethaby and Skidmore [10] for impact of thin steel plates by blunt steel missiles. For ductile metals, the process of dishing is predominantly plastic in nature, and for missiles which perforate the plate at impact velocities near the ballistic limit, it can account for a large proportion of the total energy absorbed. We have seen that the impact of thin polycarbonate plates is again accompanied by a pronounced dishing process, which also accounts for the majority of the energy absorption. However, the much larger yield strain of the polymer results in the dishing being almost entirely elastic in nature.

The final failure of dished metal plates occurs either by petalling or plugging, depending on factors such as the missile nose shape. Petalling has been observed by a number of authors including Calder and Goldsmith [5] and Landkof and Goldsmith [11]. Calder and Goldsmith [5] observed petalling of thin aluminium plates impacted by cylindro-conical missiles but the failure mode for the impact by spheres and blunt missiles was that of plugging. These responses are similar to those reported in this paper for polycarbonate, except that the spherical missile leads to petalling of polycarbonate plates. Additionally, the failure mode of thin polycarbonate plates impacted by blunt missiles appears to be more one of brittle cracking rather than a shear plugging mode. Palomby and Stronge [6] report that discing (in plane stretching leading to tensile failure near the periphery of the impact site) occurs for the impact of thin steel plates by blunt missiles. In the case of polycarbonate, only thin plates perforated by flat nosed missiles exhibit discing.

The penetration of thick metal plates generally occurs by plugging rather than the axisymmetric expansion deep penetration process observed for polycarbonate. When a cavitation process is established in metals, as may occur for impact by ogival tipped missiles, the hole produced in the plate behind the missile is often larger than that of the missile itself [12]. The enlarged hole is caused by the inertia of the plate material moving in the radial direction, and hence is more likely to be observed in materials of low specific yield strength. The yield strains of metals is small (of the order of 0.1%), whereas the yield strain of polycarbonate is large (of the order of 5–10%). Hence the elastic recovery of polycarbonate after perforation is much larger than that of metals.

6. CONCLUSION

Ballistic tests have been conducted with 7 mm diameter missiles of both spherical and flat nosed cylindrical shape, and with plate thicknesses of 2, 5 and 12 mm. Five main types

of plate behaviour have been identified. They are elastic dishing, petalling, deep penetration, cone cracking and plugging. Petalling is the mode of failure of all thicknesses of plate perforated by spherical missiles, and is preceded by elastic dishing for thin plates. Cone cracking is the mode of failure of thin and intermediate thickness plates impacted by cylindrical missiles. Deep penetration is the process by which missiles of both shapes penetrate the thick plates. Plugging is the mode of final failure of thick plates impacted by cylindrical missiles.

Acknowledgement—The authors wish to thank the Science and Engineering Research Council and the Stores and Clothing Research and Development Establishment (MOD) for the funding of this work under contract number GR/E 22428.

REFERENCES

1. J. RADIN and W. GOLDSMITH, Normal missile penetration and perforation of layered plates. *Int. J. Impact Engng* **7**, 229–259 (1988).
2. S. C. WRIGHT, Y. HUANG and N. A. FLECK, Deep penetration of polycarbonate by a cylindrical indenter. Submitted to *Mechs. Mater.* (1992).
3. N. A. FLECK, W. J. STRONGE and J. H. LIU, High strain rate shear response of polycarbonate and polymethyl methacrylate. *Proc. Roy. Soc. Lond.* **A429**, 459–479 (1990).
4. S. C. WRIGHT, High strain rate response and ballistic impact of Polycarbonate. PhD. Thesis, Cambridge University (1991).
5. C. A. CALDER and W. GOLDSMITH, Plastic deformation and perforation of thin plates resulting from missile impact. *Int. J. Solids Struct.* **7**, 863–881 (1971).
6. C. PALOMBY and W. J. STRONGE, Blunt missile perforation of thin plates and shells by discing. *Int. J. Impact Engng* **7**, 85–100 (1988).
7. R. S. J. CORRAN, P. J. SHADBOLT and C. RUIZ, Impact loading of plates—an experimental investigation. *Int. J. Impact Engng* **1**, 3–22 (1983).
8. A. I. O. ZAID and F. W. TRAVIS, A comparison of single and multiplate shields subjected to impact by a high speed projectile. *Conf. Mechanical Properties at High Rates of Strain* (edited by J. Harding), pp. 417–428. Institute of Physics, London (1974).
9. W. GOLDSMITH and S. A. FINNEGAN, Penetration and perforation processes in metal plates at and above ballistic velocities. *Int. J. Mech. Sci.* **13**, 843–866 (1971).
10. J. W. LETHABY and I. C. SKIDMORE, The deformation and plugging of thin plates by missile impact. *Proc. Mech. Properties at High Rates of Strain* (edited by J. Harding), 2–4 April, 1974. Institute of Physics, Oxford (1974).
11. B. LANDKOF and W. GOLDSMITH, Petalling of thin, metallic plates during penetration by cylindro-conical missiles. *Int. J. Solids Struct.* **21**, 245–266 (1985).
12. R. Hill, Cavitation and the influence of headshape in attack of thick plates by non-deforming missiles. *J. Mech. Phys. Solids* **28**, 249–263 (1980).
13. M. LANGSETH and P. K. LARSEN, Dropped objects' plugging capacity of steel plates: an experimental investigation. *Int. J. Impact Engng* **9**, 289–316 (1990).
14. S. C. WRIGHT, Techniques employed to study the impact behaviour of Polycarbonate—the ballistic impact test rig at C.U.E.D., Technical report CUED/C-MATS/TR.172 January 1990, Cambridge University Engineering Department (1990).